

LA-11956-MS

UC-706 and UC-741  
Issued: December 1990

LA--11956-MS

DE91 004297

*A Simple Plane-Wave Explosive Lens*

J. N. Fritz



Los Alamos Los Alamos National Laboratory  
Los Alamos, New Mexico 87545

MASTER

DISTRIBUTION OF THIS DOCUMENT IS UNLIMITED

# A SIMPLE PLANE-WAVE EXPLOSIVE LENS

by

J. N. Fritz

## ABSTRACT

A simple plane-wave lens, using an inert central plastic wave shaper, has been designed. An experiment was done with a 4-in. diam, zeroth-order design. An iterative technique that uses measured time deviations to correct the next wave shape was developed. Two identical versions of the first iterated shape were fired. Arrival-time deviations in these first iterates fell within 50-ns bounds. With greater care and further iteration, lenses bound by 10-ns deviations seem possible.

## INTRODUCTION

Current explosive lenses, although successful, have problems; they tend to be expensive. Required rigid tolerances and concomitant machining costs account for much of the expense. Complex explosive formulations make uniform production difficult.

Most explosive lenses<sup>1</sup> operate by transforming the spherical wave from a single detonator to a plane wave by using a central explosive, with a slow detonation velocity, bounded by a sheath of explosive with a faster detonation velocity. For a certain sheath angle, the fast detonation velocity of the outer explosive, expanding on a spherical front, induces a flat wave in the central explosive that is moving at its detonation velocity. Using an explosive for the central part of the lens is an advantage because the detonation velocity,  $D$ , is not diminished by attenuations coming from the rear of the lens. The faster external explosive usually overdrives the internal explosive. This again should result in a relatively constant  $D$ , because the tangent Chapman-Jouget condition implies a slowly varying  $D$  for relatively wide-pressure excursions. A slow detonation velocity for the inner explosive results in a wide aspect for the lens ( $D_{in}/D_{out} = \cos \Theta$ , where  $\Theta$  is the half angle of the outer sheath). This allows the use of a minimal amount of the high-detonation velocity (and usually more energetic) explosive, which is an advantage. Baratol, a TNT/Ba (NO<sub>3</sub>)<sub>2</sub> mixture, served this purpose admirably in the old P-xx lenses. It is now deemed a hazardous waste because of the barium content. Currently, a mixture of TNT/CaCO<sub>3</sub>/microballoons/talc is replacing Baratol.

Another way<sup>2</sup> of delaying the central dome of the spherical wave is to use an air gap. A donor explosive accelerates a metal plate. The shaped metal runs through the gap and lands simultaneously on a flat acceptor explosive. Because of the large difference between the free-surface velocity of the metal and detonation velocity in explosives, tolerances in shapes and positioning of the components of the lens are extremely tight.

The design for a lens we present here is directed toward simplicity and economy. We present the results of preliminary designs and experiments.

## THE BASIC IDEA

Our idea for a lens is shown in Fig. 1. We use an inert material instead of an explosive for the central wave-shaping mechanism. All of the complicated machining is concentrated in the curved surface of part B. Once a shape has been finally determined, this part could be fabricated by molding a suitable plastic. A final bit of machining would probably be required to make the shape true.

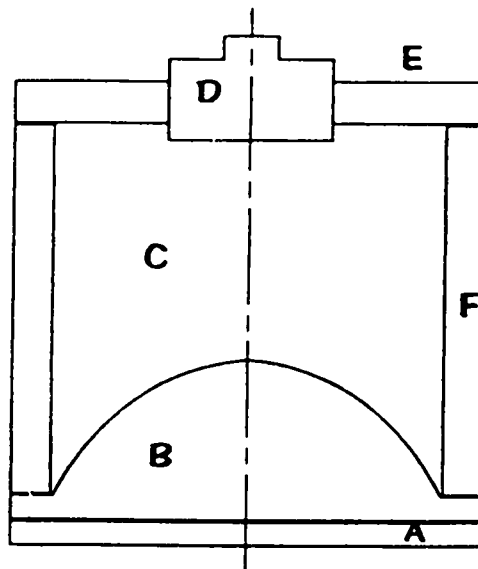


Fig. 1. Schematic of Lens. A - acceptor explosive, B - plastic wave shaper, C - donor explosive, D - detonator, E - detonator support and lid for explosive, F - plastic cylinder to hold in explosive.

For the donor explosive, we envision a material that can be poured or pressed into the lens and, in this process, conform to the shape of part B. Liquid TNT could be poured into the donor explosive cavity. A plastic capable of withstanding this temperature and chemical environment is doubtless available. One should try to match thermal expansions of the explosive and plastic. This is presumably an easy job since they are "similar" organic materials. Freezing of the liquid TNT should be by thermal conduction through the flat face of part B. The practicality of this needs to be investigated.

In a lens of this type, where precise timing depends on constant material properties, it is important to choose materials that lend themselves to tight specifications. An explosive with a single chemical component such as TNT (almost a single component) has an advantage in this respect. Some of the consistent, modern, pelletized explosives, with their excellent pressing properties, are also candidates for the donor explosive.

Simple design for preliminary experiments dictated a cylinder for part F. Much of the upper explosive in the outer run is probably unnecessary. A cone, or some other shape that minimizes the upper explosive, could be used. This would also depend on how the donor explosive is packed.

For our preliminary experiments we used composition C-4 for the donor explosive and PMMA (polymethylmethacrylate-Plexiglas) for the plastic parts. A thin layer of PBX 9501 was used as an acceptor. The detonation wave in the acceptor transmitted a shock through a thin layer of Al. Arrival times over the face of the lens were recorded by flash gaps on the other side of the Al. The preliminary design used a simple lens formula and ray tracing, with constant velocities for the media. An iterative procedure was then used to correct the shape of part B, using measured time deviations from planarity. In this latter procedure, everything is kept fixed except for the position of the interface between the donor explosive and part B.

## INITIAL DESIGN AND RESULT

The radius of curvature of the central part of the wave-shaping plastic can be obtained from the simple lens approximation (see Fig. 2). This approximation is valid for a small region about the optic axis where the sagittae of the arc,  $x$ , is adequately given by  $y^2/2R$ . The spherical wave from a point detonation a distance  $P$  away from the interface arrives at the interface at  $t_1$ . At a time  $\Delta t$  later, the wave at the edge of the shown arc contacts the interface. We have  $(x_P + x_R)/D = (x_R - x_Q)/u_s$ . This gives the simple lens formula  $(PD)^{-1} + (Qu_s)^{-1} = (u_s^{-1} - D^{-1})/R_L$ . To get a flat wave,  $Q = \infty$ , and we get  $R_L = P(D/u_s - 1)$ .

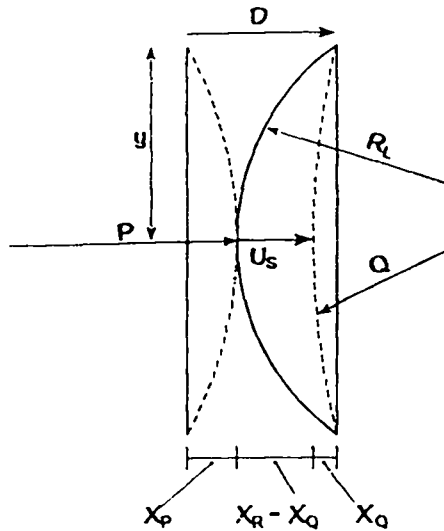


Fig. 2. Simple lens approximation for central part of lens.

We concentrate on a 4-in. diam lens, the equivalent of a P-40, with  $P = 3$  in. This is probably more explosive than is necessary on the optic axis and is a parameter to investigate in a more general study. Properties of composition C-4 explosive are not that well known. Initially, we chose  $D = 8.0$  mm/ $\mu$ s for the composition C-4 detonation velocity, and  $u_s = 6.5$  mm/ $\mu$ s for the shock velocity in PMMA resulting from the C-4/PMMA interaction. This gives  $R_L = 0.692$  in., a discouragingly small radius of curvature. However, it only applies to a small region near the optic axis. To get a better idea of our lens shape, we need to go to a ray-tracing approximation (see Fig. 3).

At  $t = 0$ , the spherical wave has just touched the plastic surface. We have at time  $t$ ,  $R(t) = P + Dt$ ,  $\Delta y = u_s t$ , and  $x^2 + (P + \Delta y)^2 = R^2$ . Hence,  $t = \Delta y/u_s$ ,  $R = P + D\Delta y/u_s$ , and  $x^2 + (P + \Delta y)^2 = (P + D\Delta y/u_s)^2$ .

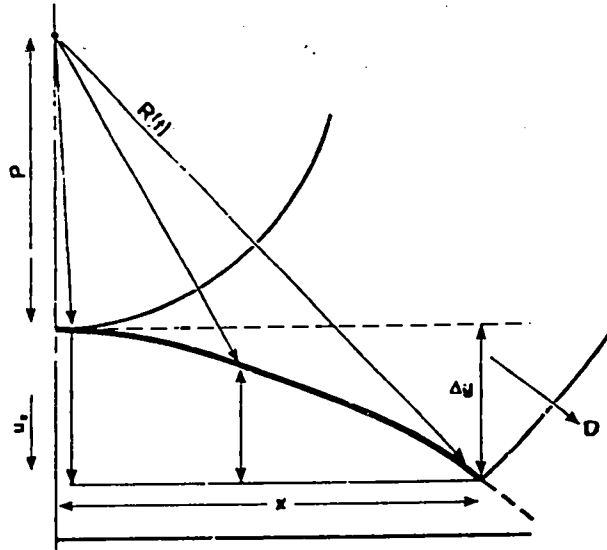


Fig. 3. Ray-tracing scheme for calculating lens shape.

We then have

$$\frac{\Delta y}{P} \left( \frac{D}{u_s} + 1 \right) = \left( 1 + \frac{D + u_s}{D - u_s} \left( \frac{x}{P} \right)^2 \right)^{1/2} - 1 \quad (1)$$

For small  $x$ ,  $\Delta y \cong \frac{1}{2} u_s x^2 / (P(D - u_s))$ . The radius of curvature is  $P(D - u_s) / u_s$ , agreeing with the simple lens approximation. For large  $x$ ,  $\Delta y \approx sx$ ,  $s = (u_s^2 / (D^2 - u_s^2))^{1/2}$ , i.e., the lens tends toward a cone, not the sphere of the simple lens approximation. For our initial numbers,  $s = 1.394$ . Figure 4 shows computed shapes using Eq. (1). For our experiment we chose  $P = 3.0$  in. A value of 2.0 in. and possibly 1.5 in. would probably have been a safe choice.

Shock velocity in the plastic is not constant. Due to the finite thickness of the donor explosive, the shock wave gradually attenuates on the optic axis after it enters the plastic. As the detonation wave moves farther on the radius of the plastic lens, the interaction between the explosive and plastic changes from normal incidence toward tangential incidence. Both of these effects cause the real wave to lag behind the calculated flat-wave position. A real detonator has finite size. We do not have an ideal point detonation. We account for this by positioning the front surface of the detonator 3/8 in. (~10 mm) nearer the plastic lens rather than at the 0-mm position of the point detonation. This number was chosen somewhat arbitrarily. One could do better by considering the actual shape of a detonator and its internal construction.

Because of perturbations and uncertainty in the properties of C-4 explosive, we need data from an experiment. Figure 5 gives our exact initial configuration. We do not expect success on the first try. The measured  $\delta t$  will be used to estimate the correction  $\delta y$ . We will keep everything in the configuration constant except for the upper shape of the plastic lens.

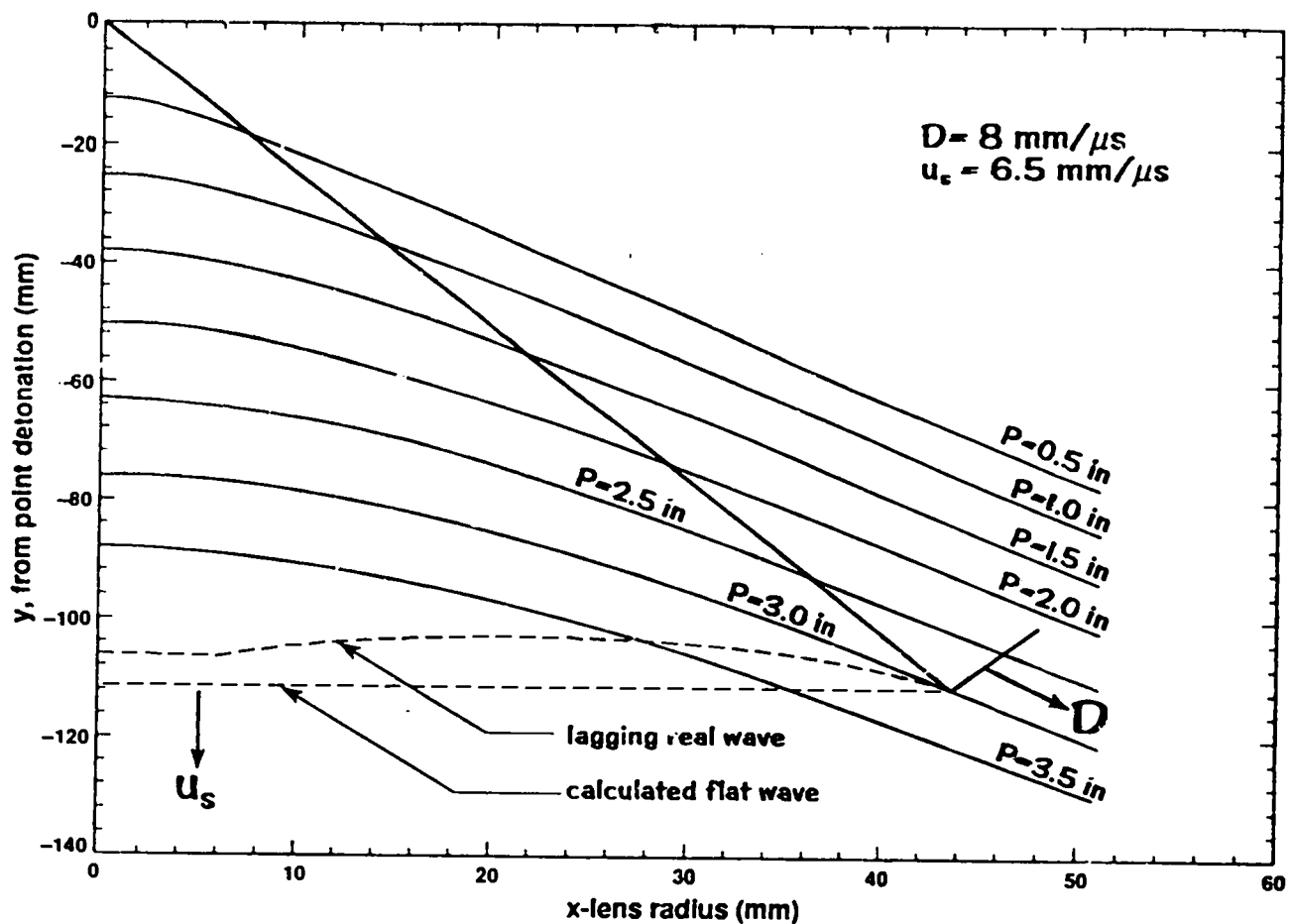


Fig. 4. Plastic lens shapes at varying explosive thicknesses from a point detonation. Note that the vertical scale is compressed by about a third.

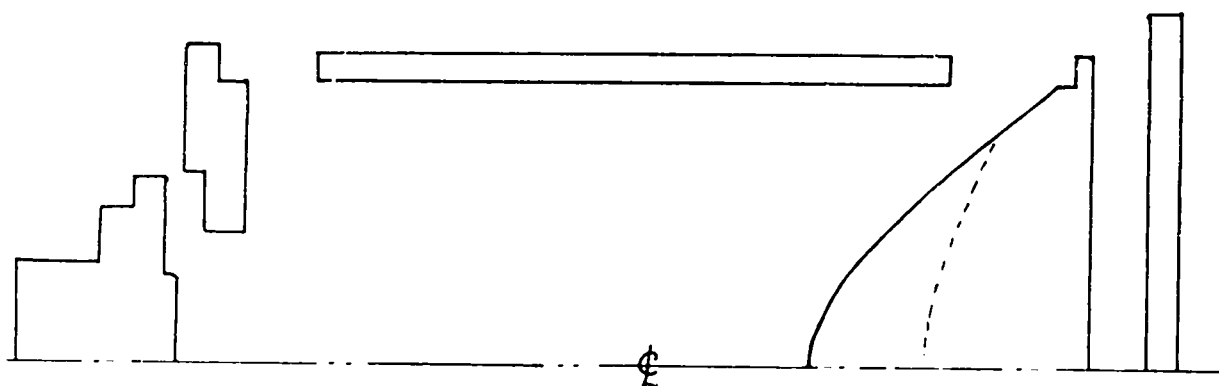


Fig. 5. An exploded view of our first design. The pieces are drawn approximately to scale. The dotted line indicates the correction made for the second design.

Seven slits, spaced 0.5-in. apart, recorded the arrival of the shock on the surface of the aluminum. Figure 6 shows the streak-camera record obtained. The axial symmetry of the lens is evident. The slit plate was not quite centered on the lens, evidenced by the pattern of peak-lags from the traces shown in Fig. 7. This affects the side traces, but has a negligible effect on the central trace. The resulting time-lags for various regions

of the lens are shown in Fig. 7. The radial location of a time-lag is obtained from the image magnification. The film may have been read slightly tilted; there were not any good streaks to align the time-axis on the film. The effect of this angle error ( $\cos \Theta$  type) on our results is negligible.

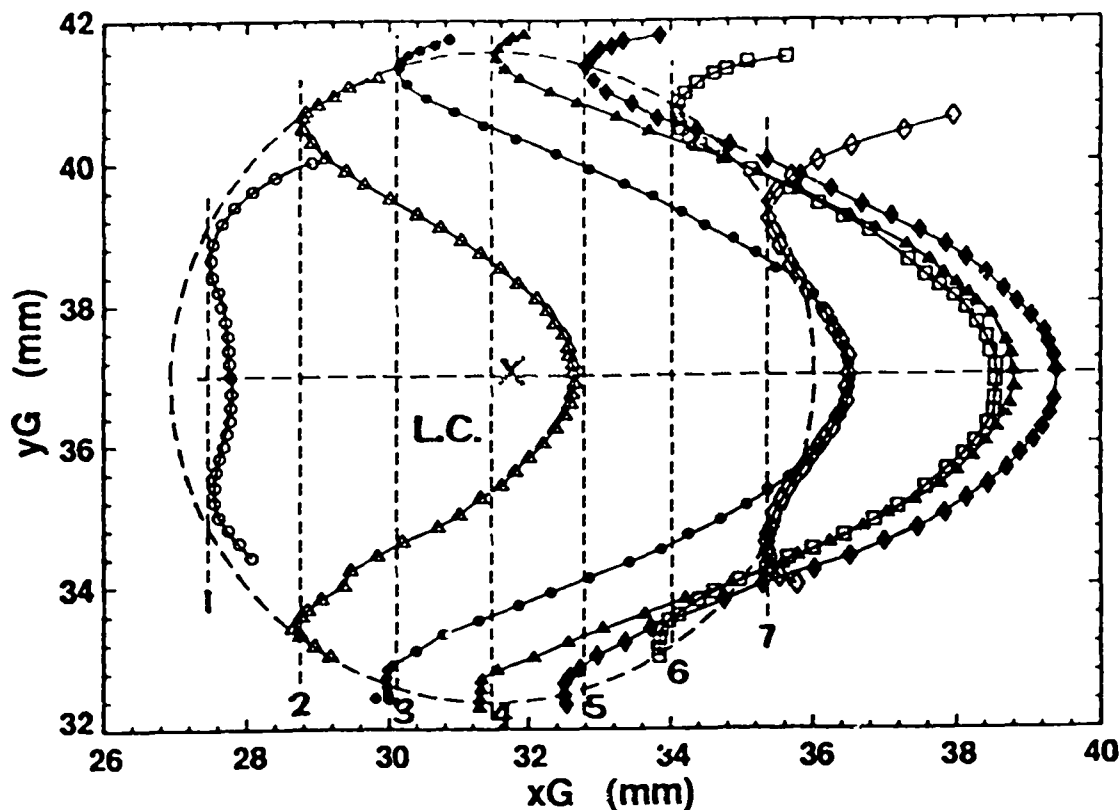


Fig. 6. Streak camera record, lens 1. Seven traces, 0.5-in. apart, record light from the flash gaps above the aluminum surface. If the record had not been swept in the x-direction ( $9.48 \text{ mm}/\mu\text{s}$ ), the traces would all have fallen on the dotted lines. The x-displacement of the trace, from the dotted lines, yields the time-lag for the wave arrival. The spacing between the dotted lines ( $1.313 \text{ mm}/0.5 \text{ in.}$ ) gives the magnification for the image,  $0.1034 (\pm 1\%)$ .

We had a time differential of  $0.80 \mu\text{s}$ . The lag was probably due to the expected attenuation caused by the Taylor wave and, in part, to our uncertainty for the value of  $Du_s/(D-u_s)$ . Our guess for this value is  $34.7 \text{ mm}/\mu\text{s}$ . On a more positive note, the traces are very smooth. The scatter about a given trace is  $\sim 20 \text{ ns}$ . If we want to control the lag time,  $\delta t$ , by moving the interface,  $\delta y$ , the "velocity"  $\delta y/\delta t \cong Du_s/(D-u_s)$  is pertinent. The value  $34 \text{ mm}/\mu\text{s}$  implies a tolerance of  $1.5 \text{ mm}/50 \text{ ns}$ . That is, for a relatively low tolerance, we have a tight control on the timing. The lag measured in the first experiment implies we have to "scalp" our lens by about an inch. This greatly improves our aspect ratio and will ultimately allow use of less donor explosive.

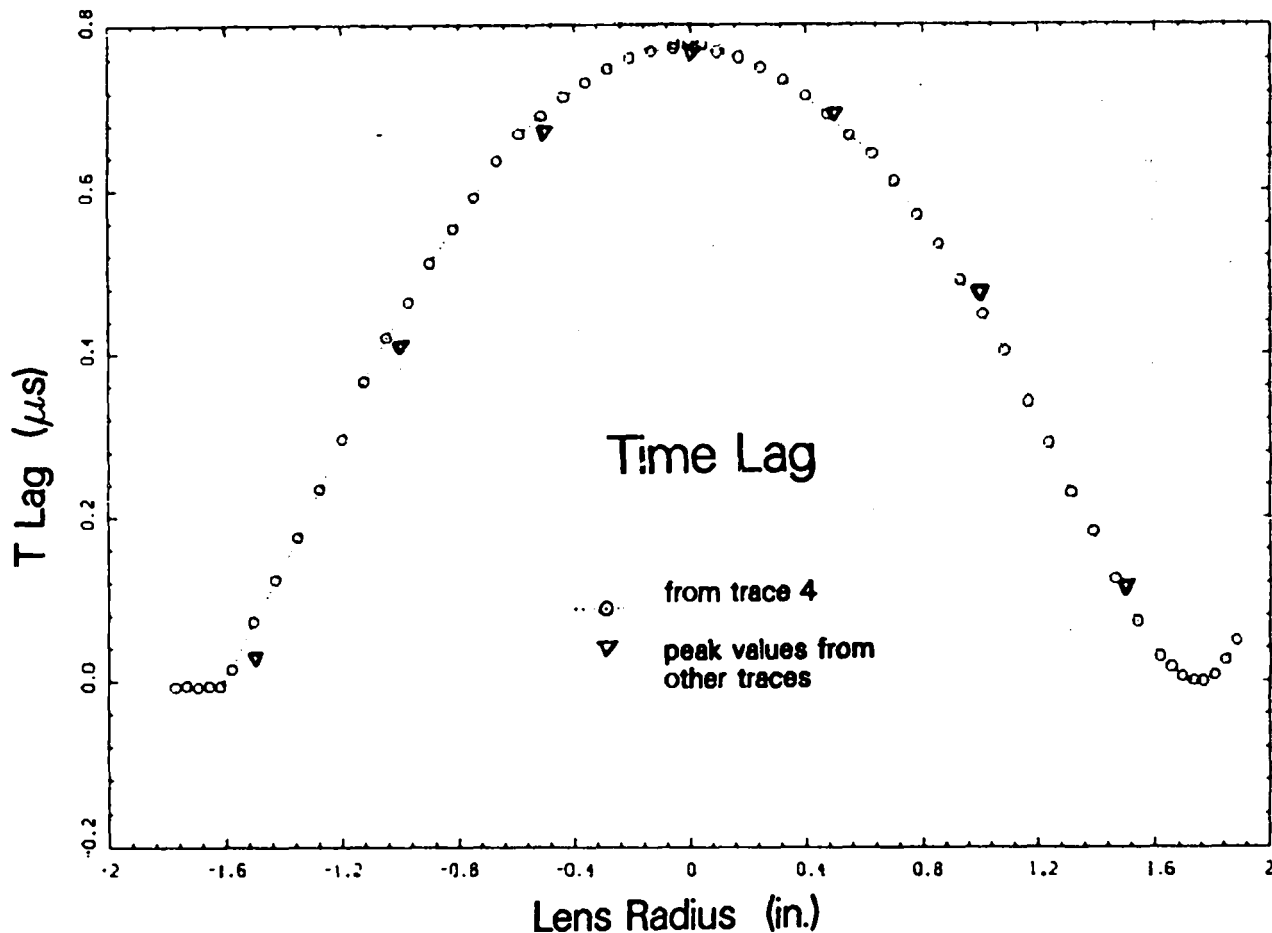


Fig. 7. Lens 1 time-lags.

The edge of the donor explosive is a sharp-edged cone pointing toward the acceptor through 0.25 in. of plastic. At this point, a side rarefaction starts working inward toward the center, relieving the wave and causing a lag in time. This influence is clearly shown in Figs. 6 and 7. The influence extends inward to a radius of 1.6 in. and 1.7 in. (definitely). A 45° rule, for loss due to unsupported plastic run, seems to be in effect. If we wanted a full 2-in. radius of flat wave, we would clearly have to extend the explosive radius to 2 in. + thickness of plastic run.

## DESIGN TWO AND RESULTS

We pay more attention to the equation of state of composition C (C-4) and PMMA. We have<sup>3</sup> for C-4,

$$\rho_o = 1.66 \text{ g/cm}^3, \quad D = 8.37 \text{ mm}/\mu\text{s}, \quad \text{and} \quad P_{CJ} = 25.7 \text{ GPa (calc.)}$$

We fit a simple  $\gamma$ -law EOS (4) to the parameters,

$$\gamma_G = \frac{\rho_o D^2}{P_{CJ}} - 2 = 2.5251 \quad \text{and} \quad q = -\frac{D^2}{2\gamma_G(\gamma_G + 2)} = -3.0656 \text{ J/mg}$$



The M-6 fit is used for the EOS of PMMA,

$$\rho_o = 1.186 \text{ g/cm}^3, \quad u_s = 2.598 + 1.516 u_p \text{ mm}/\mu\text{s}, \quad \gamma_G = 1.5.$$

We used this data and the ray-tracing code MACRAME to calculate the 1D behavior of the lens along its central axis. Results are shown in Figs. 8-11. The time-lag measured in the experiment can be attributed to the lag produced by the decaying wave in the PMMA. The inert, mock-explosive Hugoniot gave the initial pressure in the explosive as 140 kbar. This was sufficient to insure prompt initiation, with a run to detonation of <0.1 mm, in the PBX 9501 acceptor. The ability of the plastic at state B to initiate the acceptor is an important consideration in lens design. This assures a uniform pressure wave is transmitted into the adjacent material.

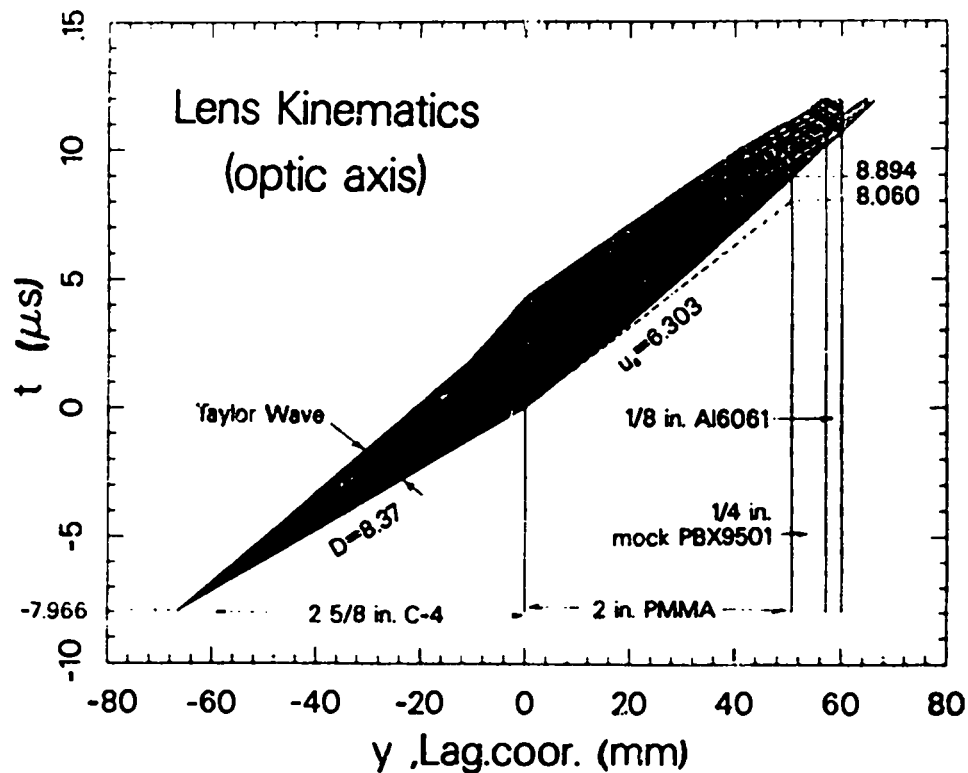


Fig. 8. MACRAME (a 1D, wave-approximation hydrocode) waves and interfaces along the lens axis (the "optical" axis). The Taylor wave emanating from the point detonation is truncated to the portion that controls the lens behavior. The decay of the shock as it travels through the plastic leads to an arrival time at the acceptor explosive 0.834  $\mu\text{s}$  later than the arrival of a nondecaying wave. We use mock explosive (a Hugoniot curve of an inert chemical match to PBX 9501,  $\rho_o = 1.87 \text{ g/cm}^3$ ,  $u_s = 2.71 + 1.61 u_p$ ,  $\gamma_G = 1.5$ ) for two reasons. First, the initial pressure in the mock Hugoniot lets us judge the likelihood of and run to detonation of the acceptor explosive. Second, MACRAME, at the moment, does not correctly handle an explosive that has been shocked to a weak detonation.

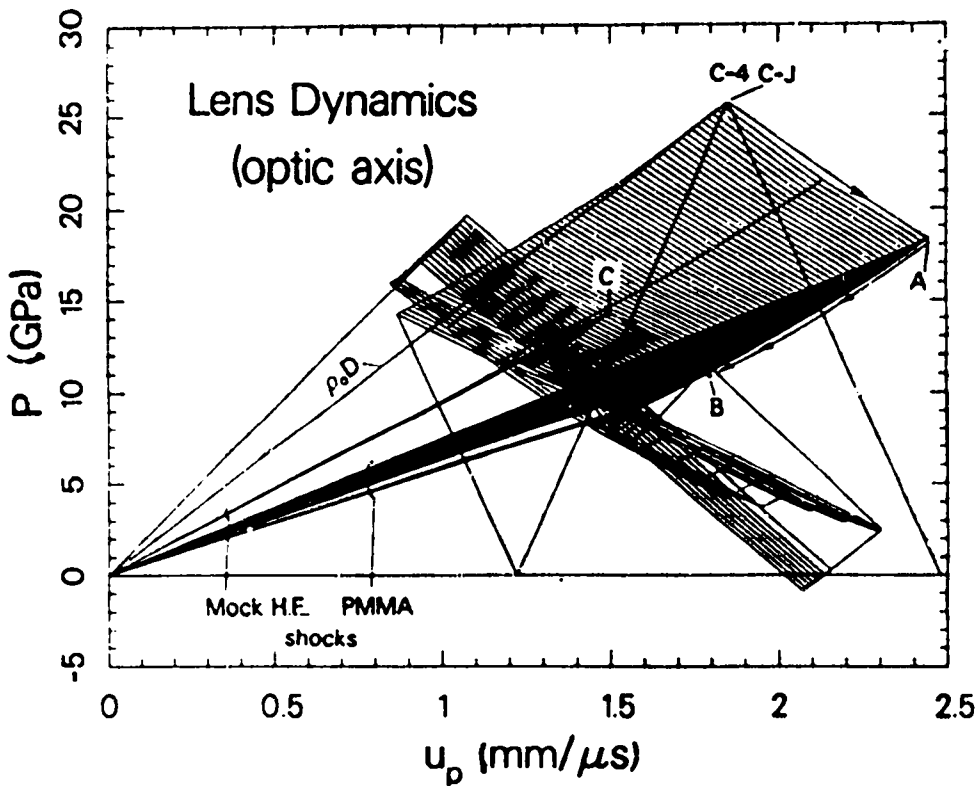


Fig. 9. MACRAME  $P - u_p$  interactions. The C-4 explosive, at its C-J point, interacts with PMMA to produce state A. As the wavelets in the explosive Taylor wave catch up to the lead shock in the PMMA, its strength decays to state B. This state interacts with the mock-explosive Hugoniot to get state C.

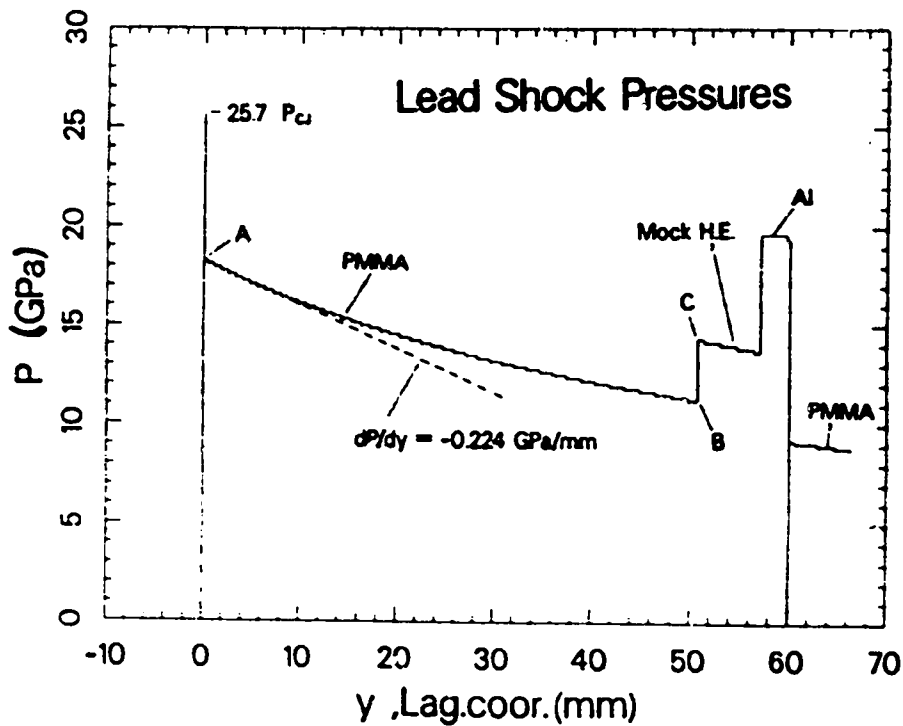


Fig. 10. Lead characteristic pressures. Pressure along the lead shock down the central axis of the lens are shown. States A, B, and C in the  $P - u_p$  diagram are indicated. In the actual lens, state C rapidly grows to a detonation in the acceptor explosive.

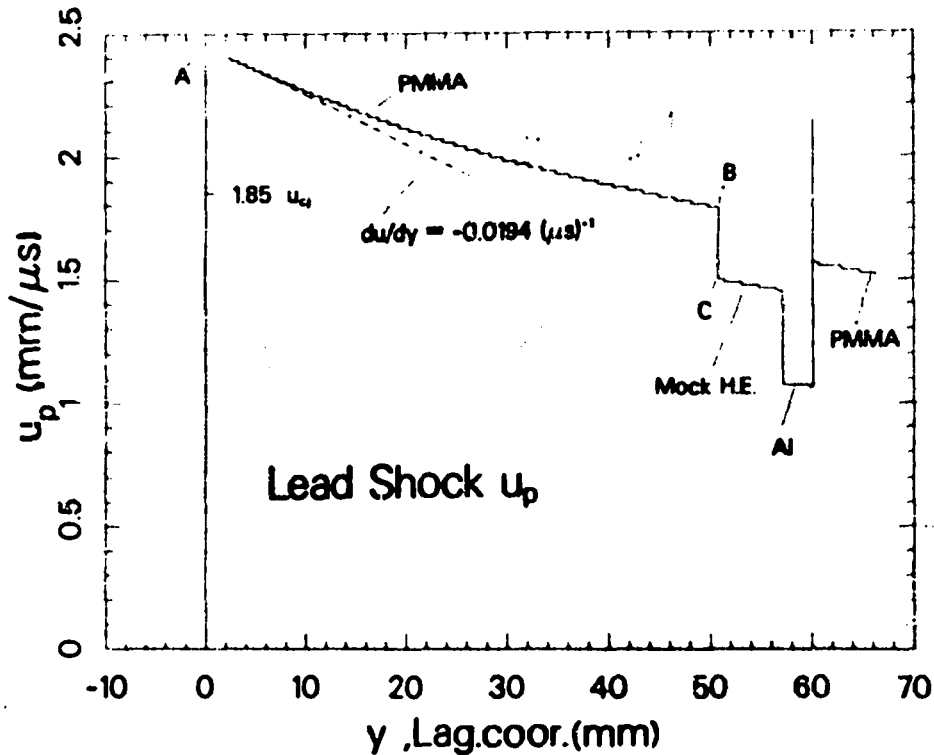


Fig. 11. Lead characteristic particle velocities.

Clearly, if we had allowed for the lag in the plastic, we would have achieved a much better 0<sup>th</sup>-order lens. We need an iterative method to go from measured time-lags,  $\delta t$ , to corrections in the explosive/plastic interface location,  $\delta y$ . We use the ray-tracing approximation. In Fig. 3, we let  $y_0$  be the thickness of the lens at the center (i.e., the position where we want the wave to be flat). Then, if at a radius  $x$ , we increase  $\Delta y$ ,  $\Delta y_{i+1} = \Delta y_i + \delta y$ , the change in arrival time (an earlier arrival) will be given by

$$\delta t = \frac{R(\Delta y)}{D} + \frac{y_0 - \Delta y}{u_s} - \frac{R(\Delta y + \delta y)}{D} - \frac{y_0 - \Delta y - \delta y}{u_s}$$

To first order in  $\delta y$  we have

$$\delta t = \delta y \left( \frac{1}{u_s} - \frac{\cos \Theta}{D} \right) \quad \text{and} \quad \cos \Theta = (P + \Delta y)/R(\Delta y) \quad (2)$$

The  $(1/u_s - \cos \Theta/D)$  factor in Eq. (2) varies from 39 ns/mm on the "optic axis" to 47 ns/mm out at the edge of our particular lens.

A spline fit to the  $\delta t$  shown in Fig. 7 was mapped to  $\delta y$  via Eq. (2). The corrected lens shape is shown in Fig. 12. A quadratic fit to this result seems adequate. The machining specifications for the new lens is shown in Fig. 13.

Two lenses were fabricated with the new shape and fired. Streak-camera results are shown in Fig. 14. We did not get the middle slit centered over the lens and the slits were slightly tilted with respect to the streaking direction; however, this is not critical to the analysis. Time offsets can be measured relative to the dotted lines added to the figure.

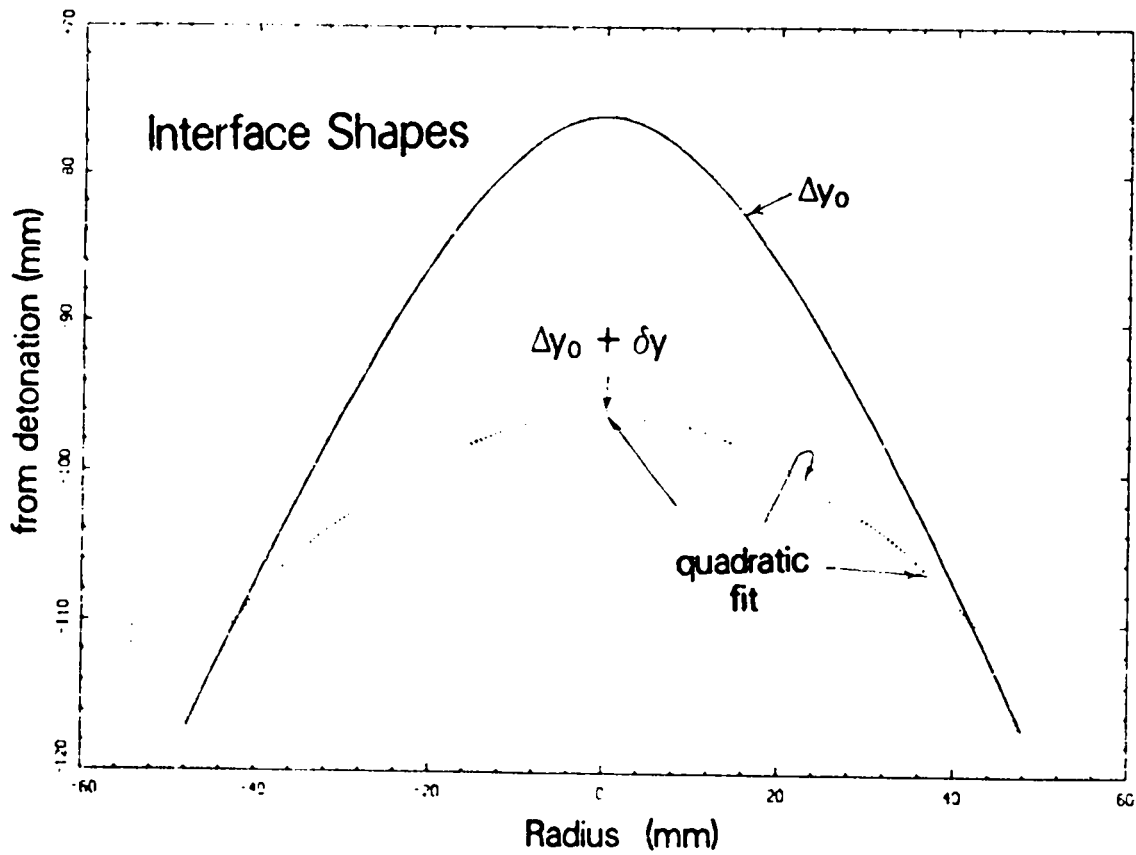


Fig. 12. New lens shape, first iteration.

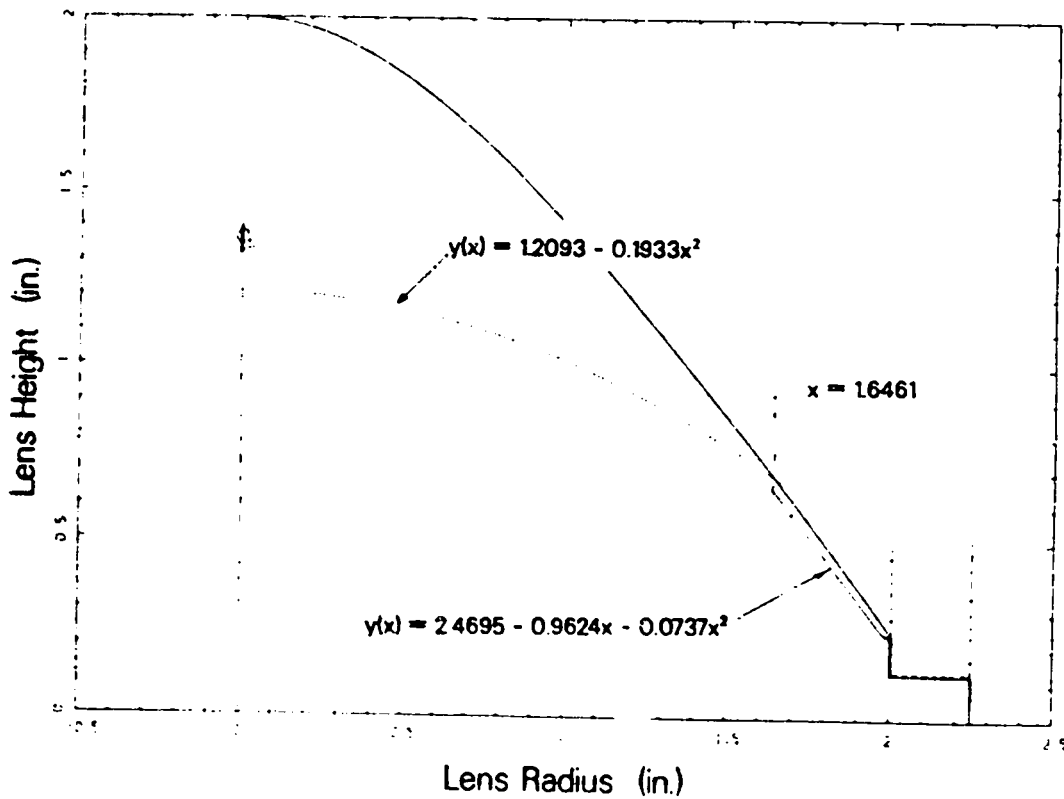


Fig. 13. Specification for lens shape (dimensions in inches).

In this particular iteration of the shape, the outer, sharp wedge of explosive still produces a circle of earliest arrival that is readily apparent in the traces. Presumably, in a final iteration, this early arrival will be lost or ambiguous. Figure 15 shows the same records with the  $x_G$  axis changed to time. Relative times along a trace are meaningful.

Figure 16 shows the  $t$ -offsets from a base, the dotted lines in Fig. 15. Lens 3 seems more evolved in the center than lens 2, but both have a characteristic "M" shape. In both cases, the arrival-time spread is about 50 ns. The character of the deviation follows the character of the deviation of our polynomial approximation, from the first calculated iterative shape. This is probably fortuitous because of the large size of our iterative first step. It does suggest that we ought to use a spline to represent our  $y$ -shapes rather than a low-order polynomial.

In Fig. 17, we plot the displaced traces (giving a 3D effect) from lens 3. The axial symmetry of the deviation from simultaneous arrival is apparent. The outer portion of the retained trace is the early arrival from the sharp wedge of explosive at the outer portion of the lens. (Actually, side rarefactions have cut into this wave and moved it in along the  $45^\circ$  line from the wedge tip.) There is a circular region of lagging arrival and then, in the center, a dome of early arrival. We should have followed the precise spline for  $\Delta y_o + \delta y$  in Fig. 12 for our machining specifications in Fig. 13! (This has to be fortuitous for such a large, first-iterative step.)

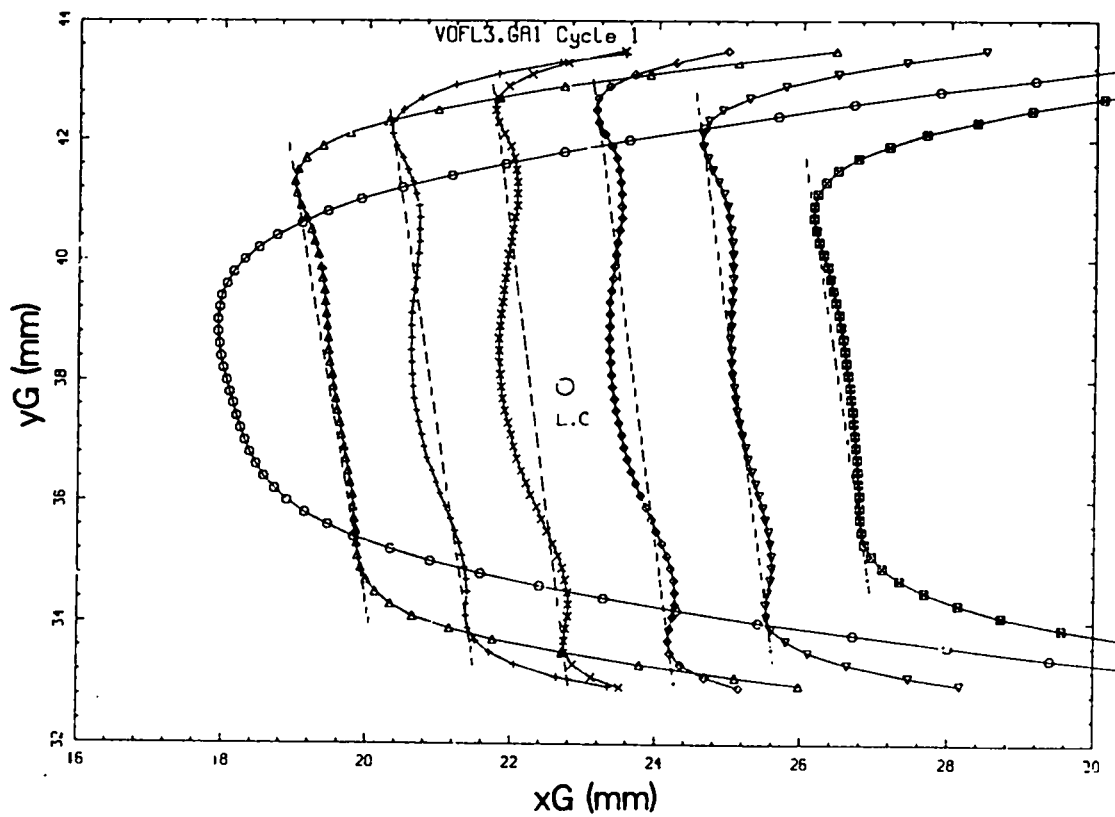
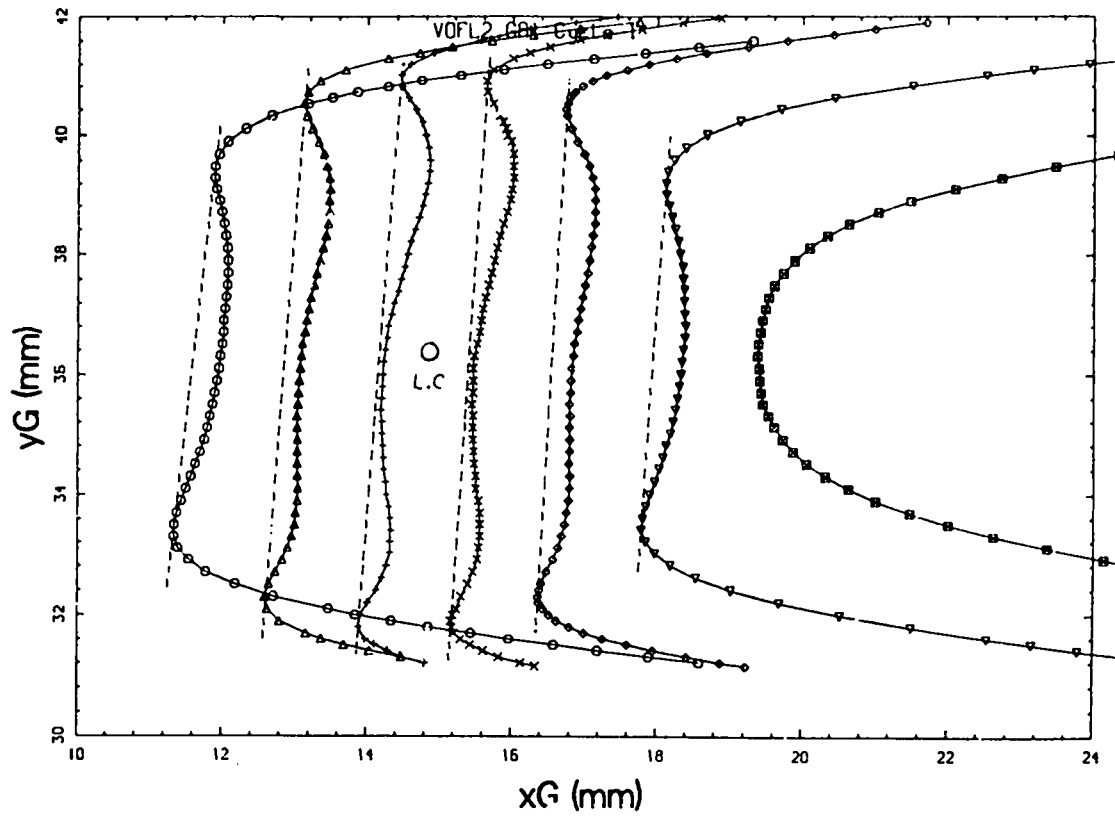


Fig. 14. Trace readings from new lens shape, (a) lens 2, (b) lens 3. The recording system is the same used for lens 1 (see Fig. 6).

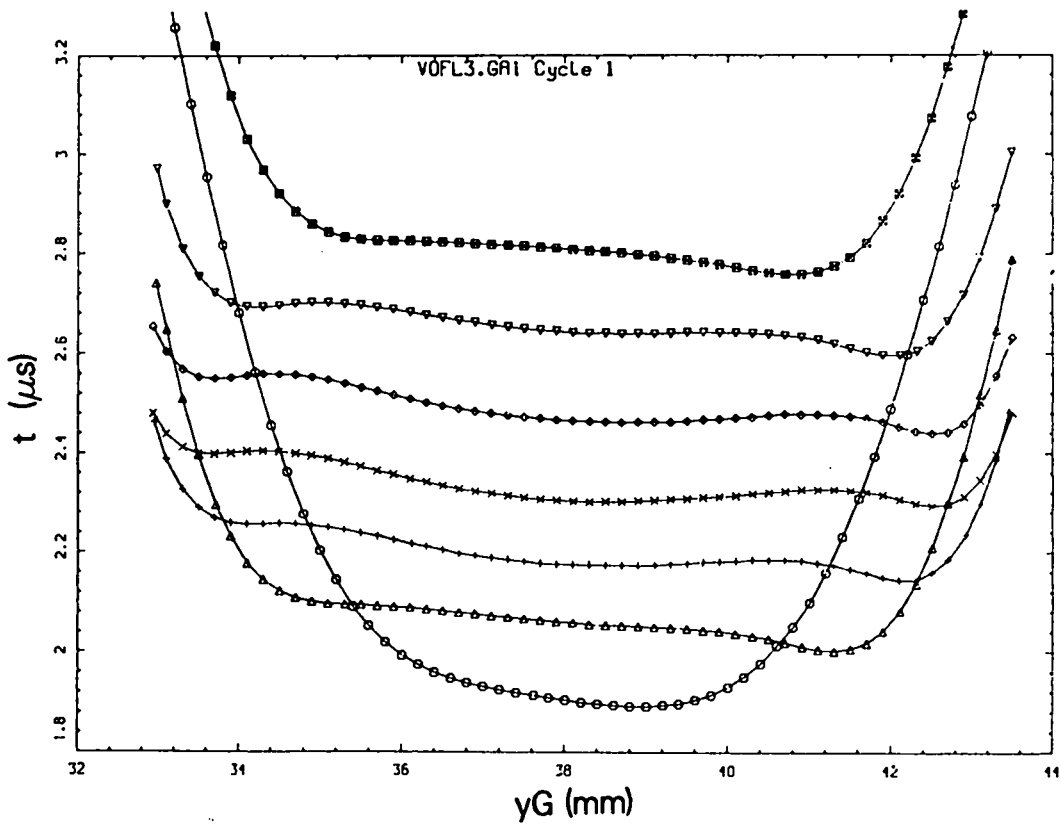
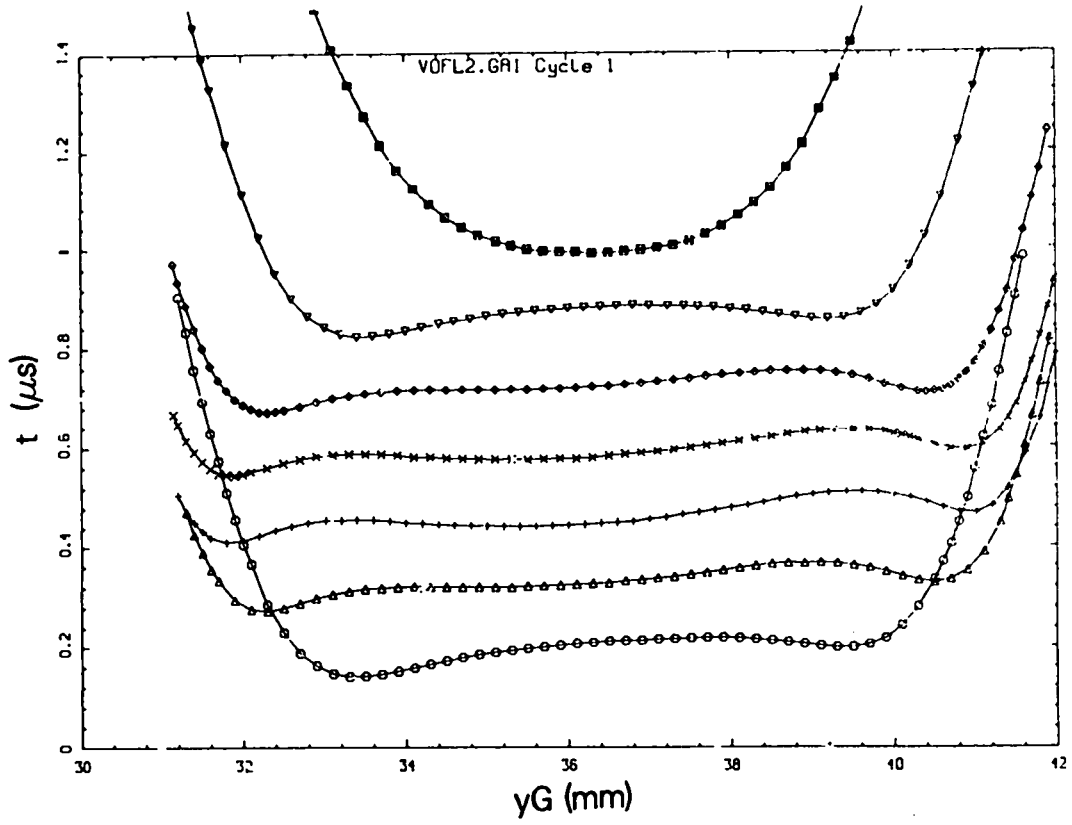


Fig. 15. Trace times vs  $y_G$ , (a) lens 2, (b) lens 3.

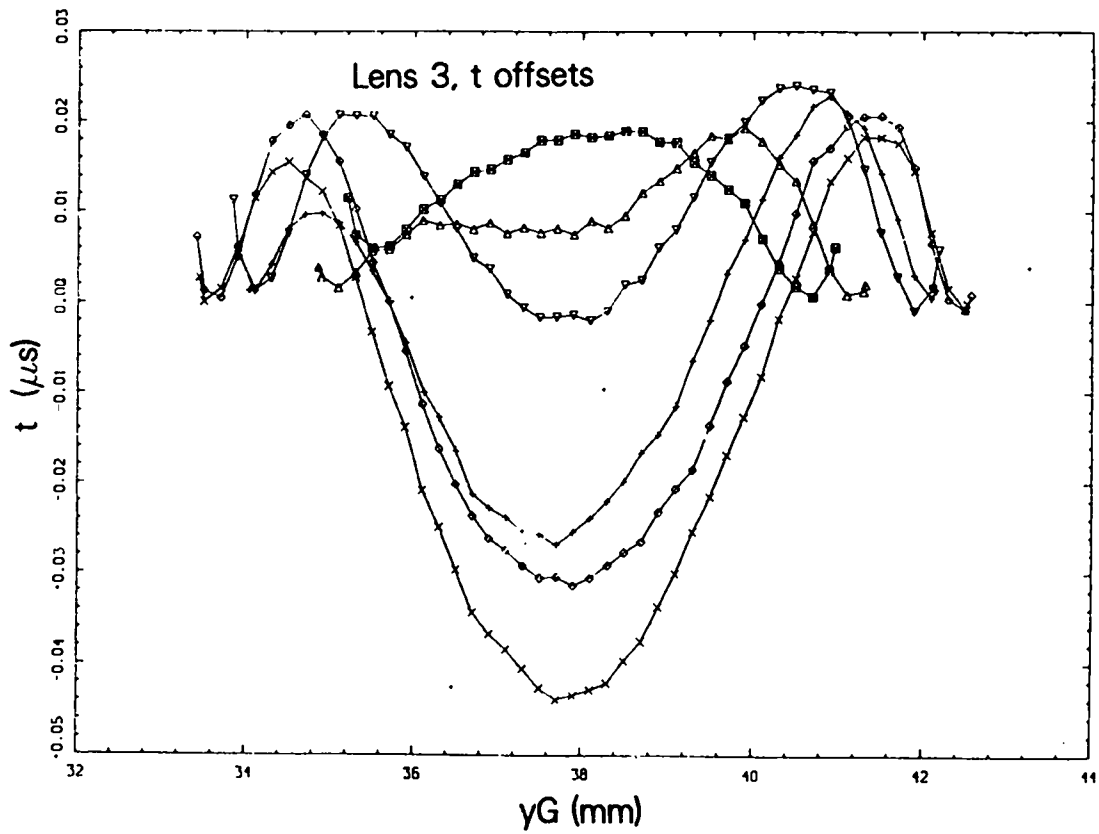
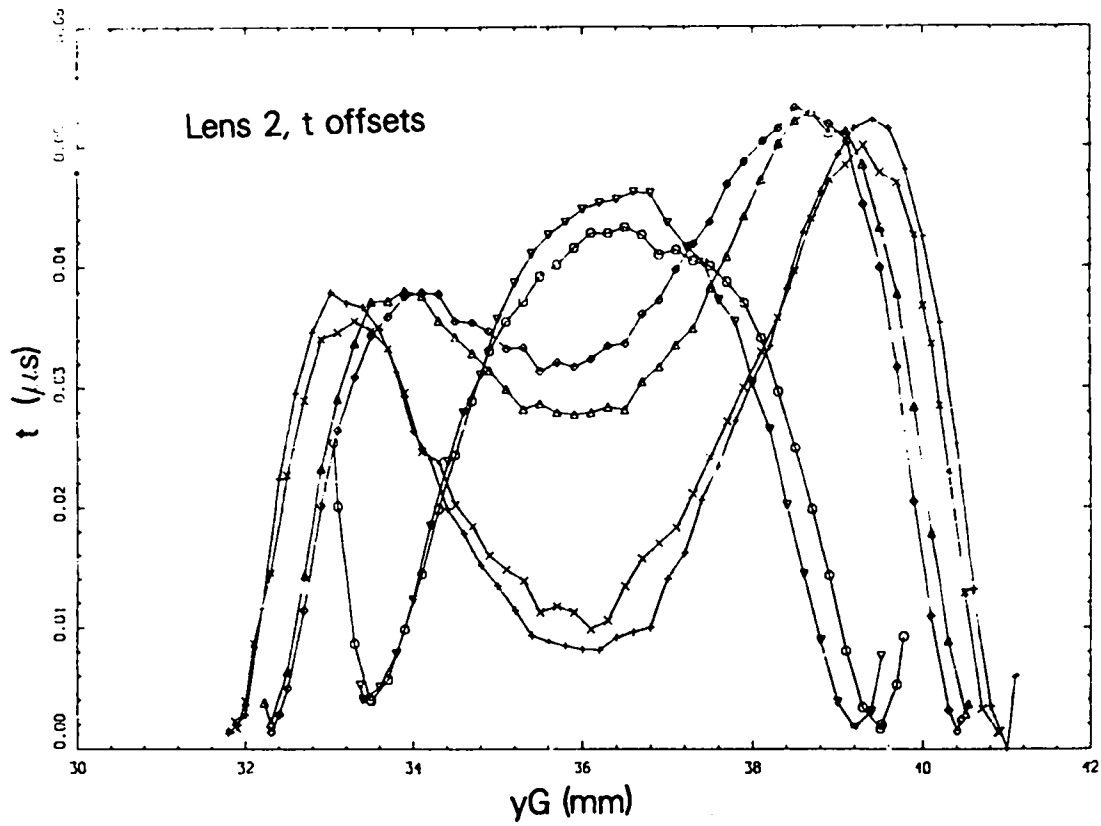


Fig. 16. Times relative to outer early circle, (a) lens 2, (b) lens 3.



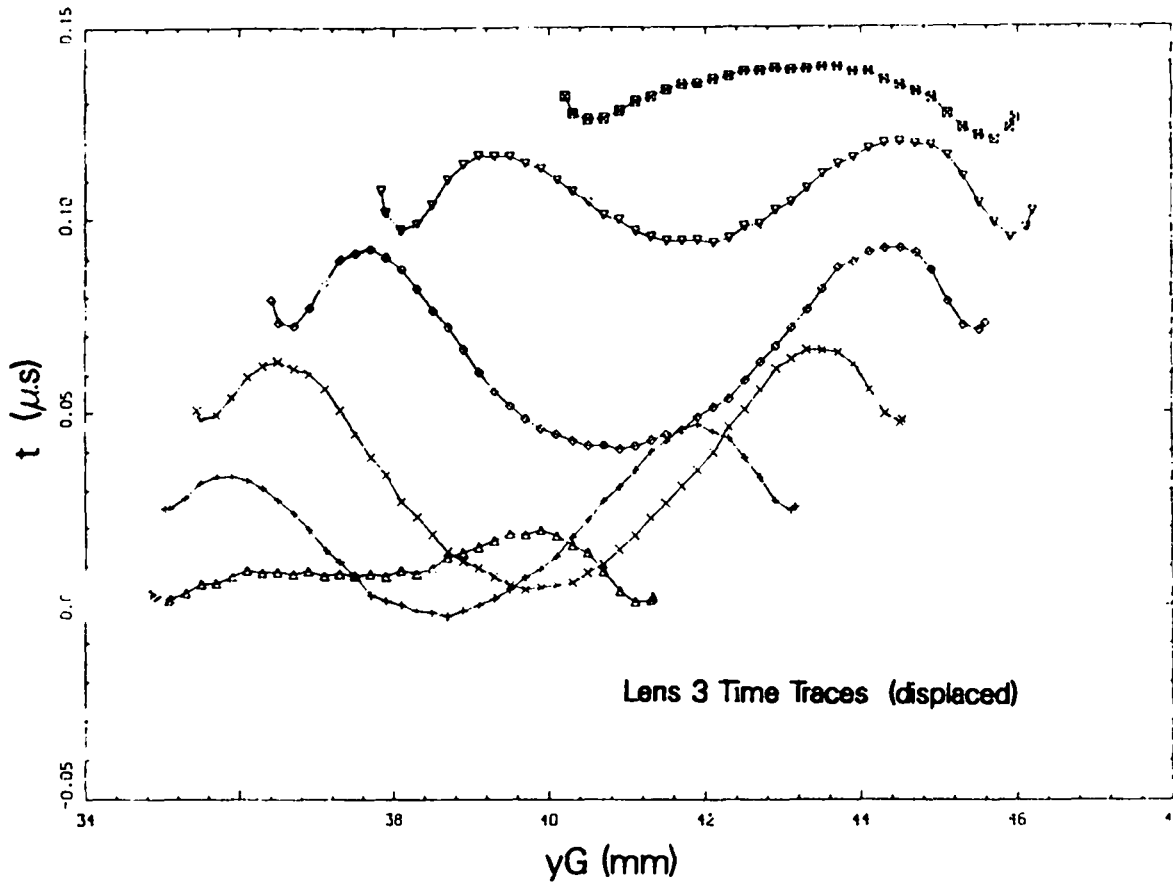


Fig. 17. Displaced  $t$ -offsets from lens 3.

## 2D CALCULATIONS

We have approximated the full 2D behavior of the lens by picking particular 1D ray paths. A full 2D calculation of our last iteration is appropriate at this point. We use a 2D Eulerian code for the task. The calculational setup is shown in Fig. 18. Pressure contours are shown in Fig. 19, when the wave has advanced about a quarter of the way into the mock-HE layer. One can tell from this picture that a fairly flat wave has been achieved. A better idea of the wave shape calculated by the 2D code can be obtained by plotting the PMMA/Mock-HE interface pressure. Figure 20 shows two times that closely follow the entry of the wave into the mock HE. This still does not give us precise, sharp, shock-wave arrival time. The difficulty is that it would take a lot of cells in the code in the vicinity of the interface to sharply define a shock. This is incommensurate (i.e., would lead to a prohibitively large calculational time) with the overall size and time required for calculating this problem. We see that we have delivered a relatively flat wave in the lateral sense. This is the information we sought from the 2D calculation of about 100 kbar. This is less than we obtained from the 1D calculation. This is because of the way the Eulerian code spreads the incoming pressure. Later, the pressure does increase to 150 kbar.

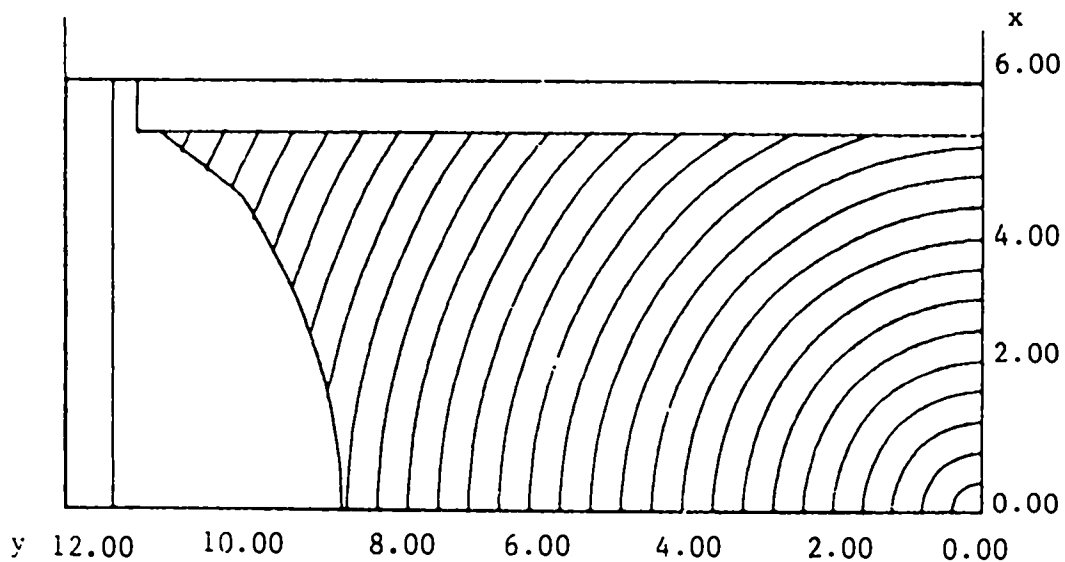


Fig. 18. Setup for calculating our last iteration for the lens. The explosive is detonated by a Huygens construction moving at the detonation velocity  $D$ . This is shown in the explosive component. Also shown are the plastic containing wall, the plastic wave shaper, and a layer of acceptor mock HE. Dimensions are given in cm.

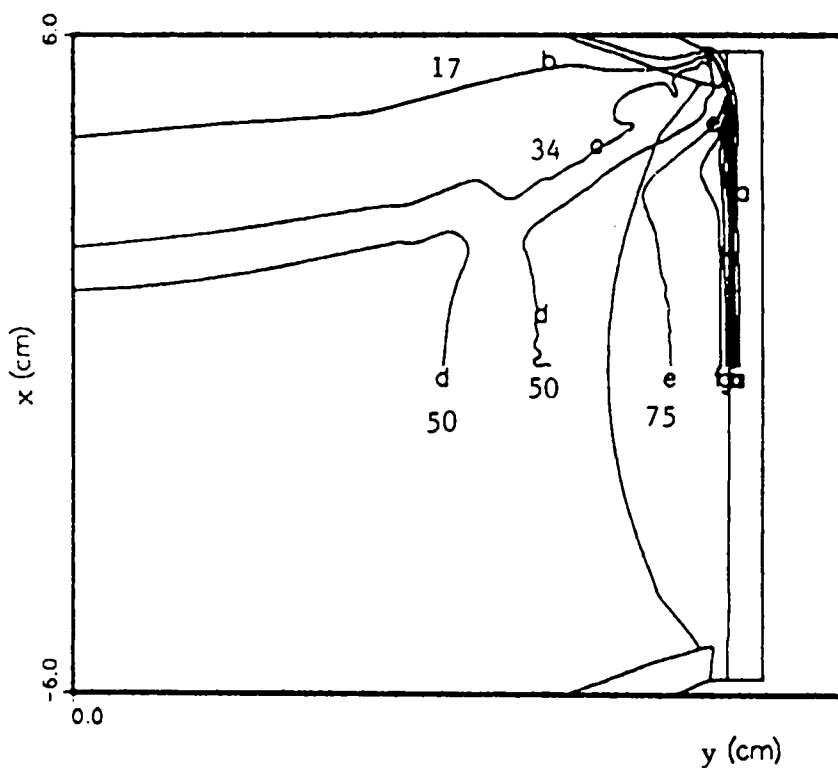


Fig. 19. Pressure contours 16.5037  $\mu$ s after the point detonation.  $a, b, c, d, e, f, g, h = 0.5, 17, 34, 50, 75, 100, 116, 133$  kbar.

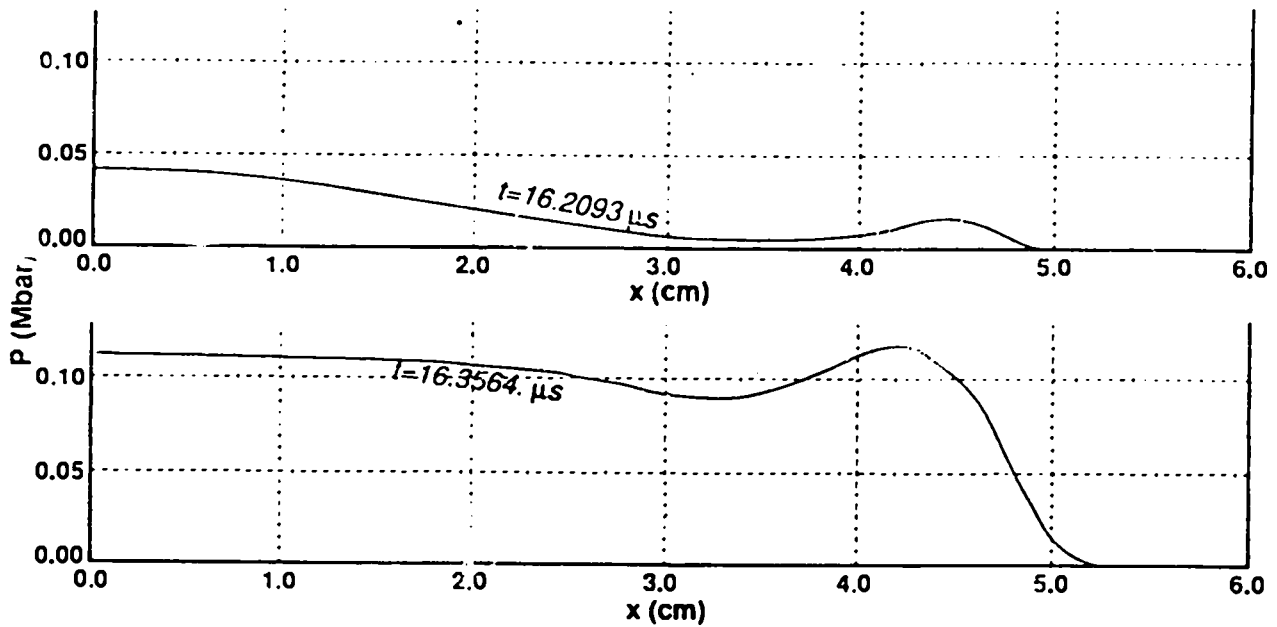


Fig. 20. Pressures at the interface between the lens and the (mock) acceptor explosive.

We give a further display of the calculation in Fig. 21. If we take the *e*-contour (sort of a half height of 50 kbar) as a representative of where the sharp shock should be, we get agreement, qualitative and quantitative, with the measured dispersion in arrival times in the experimental flash-gap analyzer.

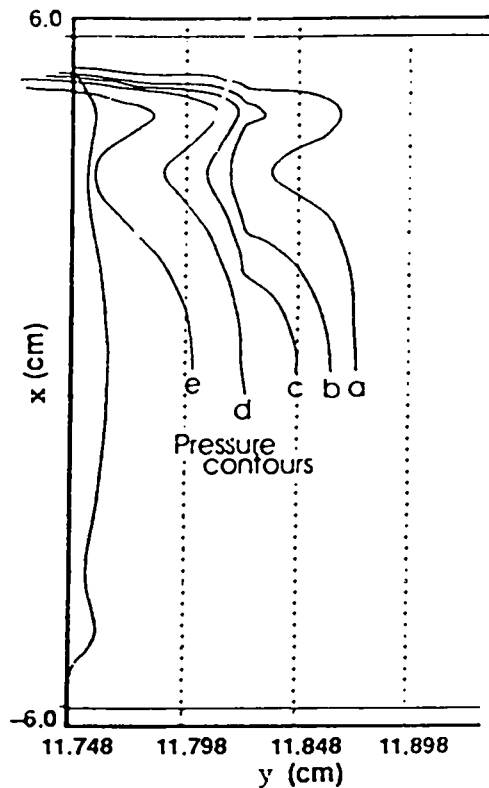


Fig. 21. Expanded version of Fig. 19; but slightly earlier,  $t = 16.3564 \mu s$ . The pressure contours in this plot are: *a, b, c, d, e* = 1, 5, 10, 20, 50 kbar. The spacing between the dotted lines (0.5 mm) corresponds to a 50-ns interval for shock transit time in the mock HE.

## DISCUSSION AND CONCLUSIONS

We stopped with this iteration. Our intent was not to perfect this particular lens system, but rather to demonstrate that this particular concept for a lens could readily be developed into a reliable and economical plane-wave lens. (The lens we arrived at on the first iteration would actually be quite useful for many applications.) Clearly, the iteration process we used removes time lead and lags in an adequate manner. We have a "coarse" and a "fine" tuning knob. The iterative process is the "fine" tuning and is a success because of the large value of the phase velocity,

$$\delta y_{\text{interface}}/\delta t = u_s D/(D - u_s) = 35 \text{ mm}/\mu\text{s} \quad .$$

We can have relatively low tolerances on  $\delta y$  and still get 10 to 20-ns limits on  $\delta t$ . The coarse knob is "keeping the rest of the lens constant." This is where troubles will come from. Fanatical quality control may be required to take full advantage of the fine-tuning capability. We have not done a "complete engineering" job on the back side of the lens. Details of the back side of the lens will affect the wave shaping in the lens. Fluctuations in these details will result in fluctuations in wave shape. The back design should minimize such transfers in the fluctuations. We have not fully explored this problem. We list some apparent advantages and disadvantages of this type of a lens.

### Advantages

- All of the expensive free-form fabrication is done on an inert material, the plastic lens.
- For production runs, a mold can be made for the plastic lens. Final machining would just be "trueing up the final shape."
- There is essentially no metal in the lens, hence no shrapnel.
- The wave is smooth; there are no small wavelength perturbations.
- Given the smoothness of the wave arrival and the fine-tuning capability, a wave arrival flat to 10 ns seems possible. Smoothness to this level will depend on reproducibility in the "back design."

### Disadvantages

- Changes in back conditions may affect wave arrival.
- The shock delivered by the flat part of the plastic lens might (depending on the explosive/plastic combination being used) be weaker than a fully explosive lens. An acceptor pad of readily detonated HE could be required as a second component of the lens.
- Such a lens will probably be bulkier than a fully explosive lens. However, it is not clear at this point as to which type would require more explosive.

- At this time, design and methods of fabrication have certainly not been completely worked out. Because we currently have successful, fully explosive lenses, this may be a fatal disadvantage. That is okay. Our intent here is to document the work done on an alternative approach.

## PRESCRIPTION FOR DESIGNING A LENS

A production model for a lens with an inert plastic center will probably not resemble our prototype in shape, choice of explosive, or choice of plastic. Accordingly, we summarize here the steps we went through (or ideally should have) with possibly helpful suggestions, mostly in the form of questions.

1. Do the complete back design. Choose the explosive plastic combination that one is going to use. Are you going to press, pour, or pack the HE? What shape do you want and what can you get for the back surface of the explosive? How do we attach the detonator? What mechanical components, if any, are necessary to hold the explosive and the lens? Are the fabrication processes easy (or possible)? How does the lens attach to the rest of the explosive assembly? We want a lens that will deliver a flat wave to a circle of radius  $x_o$ . Having gone through all this we arrive at some design, schematically shown in Fig. 22.
2. Presumably, we know the constitutive equations for the explosive and plastic. We know  $D$ . We calculate the initial interaction between the explosive and plastic and get the  $u_s$  in the plastic.
3. Pick the  $P$  dimension. We want to get it as small as possible and yet still have enough strength in the shock coming out of the bottom of the lens to promptly initiate the acceptor explosive.
4. Calculate shape 1 using Eq. (1). We calculate it so that point  $Q$  has an  $x$  sufficiently greater than  $x_o$ . Probably, we would take  $x_Q = x_o + w$ , where  $w$  is a dimension chosen large enough for mechanical stability.
5. Using some 1D hydrocode, calculate the lag,  $\delta t_{op}$ , on the optic axis due to the Taylor release wave in the explosive. We correct shape 1. We subtract from it a quadratic in  $x$  that vanishes at  $x_Q$  and has the value  $\delta y_{op} = \delta t_{op} u_s D / (D - u_s)$  at  $x = 0$ . For a small  $P$ , step 5 may require some judicious iteration to get the attenuation in the Taylor wave (a function of  $P$ ) and the calculated shift in  $y$  to be compatible.

We now have a 0<sup>th</sup>-order lens. At this point, it would be appropriate to do a 2D calculation of its behavior. If we run into some basic incompatibilities in the back design, we make suitable changes and go back to step 1. So far, this has been cheap and easy, now we need to

6. Fabricate the lens and test it. Subsequent lenses have shapes corrected by Eq. (2), which now has the iterative form

$$\delta y_{i+1} = \delta t_i u_s D / (D - u_s \cos \Theta) \quad .$$

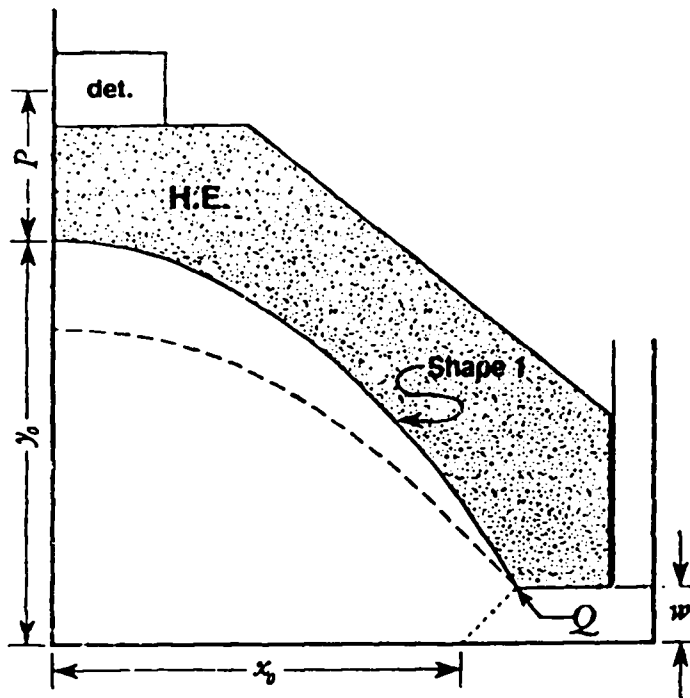


Fig. 22. Schematic of a lens design  $y_0 = \Delta y(x_Q) + w$ .

#### ACKNOWLEDGEMENT

I am indebted to J. E. Vorthman for managing the fabrication of these lenses and to S. P. Marsh for calculating the 2D behavior of the lens.

#### REFERENCES

1. J. H. Cook, "Detonating Explosive Charge and Method of Impressing Surfaces Employing Same," US Patent No. 2,604,042, July 1952.
2. S. P. Marsh, "Explosive Plane-Wave Lens," US Patent No. 4,729,318, March 1988.
3. B. M. Dobratz and P. C. Crawford, "LLNL Explosives Handbook, Properties of Chemical Explosives and Explosive Simulants," Lawrence Livermore National Laboratory, Livermore, CA, UCRL-52997 Change 2 (1985).
4. W. Fickett and W. C. Davis, "Detonation," University of California, Berkeley (1979).